IJP: Drugs and Drug Resistance 13 (2020) 28–37

Contents lists available at ScienceDirect

IJP: Drugs and Drug Resistance

journal homepage: www.elsevier.com/locate/ijpddr

MRPA-independent mechanisms of antimony resistance in *Leishmania infantum*

Noélie Douanne[a], Victoria Wagner[a], Gaetan Roy[b], Philippe Leprohon[b], Marc Ouellette[b], Christopher Fernandez-Prada[a,c,*]

[a] Département de Pathologie et Microbiologie, Faculté de Médecine Vétérinaire Université de Montréal, Saint-Hyacinthe, Québec, Canada
[b] Centre de Recherche en Infectiologie du Centre de Recherche du CHU Québec and Département de Microbiologie, Infectiologie et Immunologie, Faculté de Médecine, Université Laval, Québec, Québec, Canada
[c] Department of Microbiology and Immunology, Faculty of Medicine, McGill University, Montréal, Québec, Canada

ARTICLE INFO

Keywords:
Leishmania infantum
Antimony
Drug resistance
MRPA
Gene disruption
Whole-genome sequencing

ABSTRACT

Control of both human and canine leishmaniasis is based on a very short list of chemotherapeutic agents, headed by antimonial derivatives (Sb). The utility of these molecules is severely threatened by high rates of drug resistance. The ABC transporter MRPA is one of the few key Sb resistance proteins described to date, whose role in detoxification has been thoroughly studied in *Leishmania* parasites. Nonetheless, its rapid amplification during drug selection complicates the discovery of other mechanisms potentially involved in Sb resistance. In this study, stepwise drug-resistance selection and next-generation sequencing were combined in the search for novel Sb-resistance mechanisms deployed by parasites when MRPA is abolished by targeted gene disruption. The gene *mrpA* is not essential in *L. infantum*, and its disruption leads to an Sb hypersensitive phenotype in both promastigotes and amastigotes. Five independent $mrpA^{-/-}$ mutants were selected for antimony resistance. These mutants displayed major changes in their ploidy, as well as extrachromosomal linear amplifications of the subtelomeric region of chromosome 23, which includes the genes coding for ABCC1 and ABCC2. Overexpression of ABCC2, but not of ABCC1, resulted in increased Sb tolerance in the $mrpA^{-/-}$ mutant. SNP analyses revealed three different heterozygous mutations in the gene coding for a serine acetyltransferase (SAT) involved in *de novo* cysteine synthesis in *Leishmania*. Overexpression of sat^{Q390K}, sat^{G321R} and sat^{G325R} variants led to a 2–3.2 -fold increase in Sb resistance in $mrpA^{-/-}$ parasites. Only sat^{G321R} and sat^{G325R} induced increased Sb resistance in wild-type parasites. These results reinforce and expand knowledge on the complex nature of Sb resistance in *Leishmania* parasites.

1. Introduction

The protozoan parasite *Leishmania infantum* causes visceral leishmaniasis, a grave systemic disease that affects the spleen, liver, and bone marrow, leading to weight loss, anemia, and even death if left untreated (WHO, 2013; Sundar and Rai, 2002). *Leishmania* are intracellular parasites with a promastigote and an amastigote form, found in the sandfly vector and vertebrate host, respectively (Gazanion et al., 2016). Dogs serve as the main reservoir for infection (Abranches et al., 1991). With over 500,000 new cases of visceral leishmaniasis every year, this widespread disease is responsible for a significant health, psychosocial, and economic burden around the world (WHO, 2013; Sundar and Rai, 2002).

Leishmaniasis has long been treated with antimonial drugs; first trivalent antimonials (Sb^{III}), and later with the less toxic pentavalent antimonials (Sb^{V}) (Ouellette and Papadopoulou, 1993). The limited arsenal of available anti-leishmanial therapies coupled with the lack of an effective human vaccine make antimonials a first-line treatment still today – despite their harmful side effects (Ouellette and Papadopoulou, 1993; Papadopoulou et al., 1994; Ouellette et al., 2004). Resistance has become rampant in the field, rendering these drugs virtually ineffective against visceral leishmaniasis in certain areas of the world (Leprohon et al., 2015; Sundar et al., 2000; Rijal et al., 2003).

The mechanism of action of antimonial drugs against *Leishmania* remains ambiguous, further complicating the fight against drug resistance (Ouellette and Papadopoulou, 1993; Légaré et al., 2001;

* Corresponding author. Département de Pathologie et MicrobiologieFaculté de Médecine Vétérinaire Université de Montréal, Saint-Hyacinthe, Québec, J2S 2M2, Canada.
E-mail address: christopher.fernandez.prada@umontreal.ca (C. Fernandez-Prada).

https://doi.org/10.1016/j.ijpddr.2020.03.003
Received 8 January 2020; Received in revised form 25 March 2020; Accepted 27 March 2020
Available online 02 April 2020

Fernandez-Prada et al., 2018). Evidence suggests that pentavalent antimony (Sb^V) is actually a prodrug, reduced to the active trivalent form (Sb^{III}) in the macrophage and/or parasite (Ouellette et al., 2004). Resistance mechanisms likely rely on decreased accumulation of antimony within the parasite (either through increased efflux or reduced uptake) (Ouellette and Papadopoulou, 1993; Ouellette et al., 2004). Early experiments demonstrated the presence of an efflux pump in the membrane of *L. tarentolae* that allowed extrusion of metals conjugated to thiols, and similar systems were later observed in *L. infantum* and *L. panamensis* (Ouellette et al., 2004; Dey et al., 1996). Although metal resistance in *Leishmania* spp. is multifactorial, the ATP-binding cassette protein MRPA has been shown to be implicated through recognition of thiol-conjugated metals and subsequent sequestration near the flagellar pocket for later exocytosis and/or extrusion outside the cell (Légaré et al., 2001; El Fadili et al., 2005). Gene amplification is a frequent phenomenon in metal-resistant *Leishmania* in response to antimonial drug pressure; amplifications have been reported both intrachromosomally and as part of amplicons (Mukherjee et al., 2013; Grondin et al., 1997; Leprohon et al., 2009a; Haimeur et al., 2000). Amplifications of *mrpA*, often identified within circular amplicons in antimony-resistant strains, have been extensively characterized (Leprohon et al., 2009a; Mukherjee et al., 2007). However, while an $mrpA^{-/-}$ has been achieved in *L. tarentolae* (Papadopoulou et al., 1996), there is no available literature describing the properties of a null *mrpA* mutant in human pathogenic *Leishmania*.

The goal of this study was to complete an in-depth exploration of the effects caused by the disruption of the *mrpA* gene in *L. infantum*, including its effect on parasite survival, impact on infectivity, and response to antimony sensitivity and selection. This information is critical to being better equipped in the fight against drug-resistant *Leishmania* by furthering knowledge of one of the many mechanisms these parasites use to survive in the presence of drugs.

2. Material and methods

2.1. Leishmania cultures

Wildtype parasites (WT), as well as the different mutants (e.g. nulls and overexpressors), were cultured as promastigotes at 25 °C in SDM-79 medium supplemented with 10% heat inactivated fetal bovine serum (FBS) and 5 μg/mL hemin. THP-1 cells (ATCC T1B-202) were cultured in RPMI 1640 medium supplemented with 10% fetal bovine serum, 2 mM glutamine, 100 IU of penicillin/mL, and 100 μg of streptomycin/mL. Prior to infection, log-phase THP-1 cells were differentiated by incubation for 2 days in RMPI 1640 medium containing 20 ng/mL of phorbol myristate acetate (PMA) (Sigma).

2.2. Genomic modifications

2.2.1. mrpA null mutant

The *L. infantum mrpA* (LinJ.23.0290) null mutant ($mrpA^{-/-}$) was obtained by targeted gene replacement. *mrpA* flanking regions were amplified from *L. infantum* 263 WT genomic DNA and fused to the puromycin acetyltransferase (*puro*) gene using a PCR fusion-based method. Briefly, the 5′UTR of *mrpA* was amplified using primers MRPA_A and MRPA_B, which includes a tail of 25 nucleotides complementary to the *puro* gene (see primer sequences in Table S1). The *puro*information is critical to being better equipped ORF was amplified with primers MRPA_C and MRPA_D, which includes a tail of 25 nucleotides complementary to the 3′UTR of *mrpA*. The 3′UTR of *mrpA* was amplified using primers MRPA_E and MRPA_F. The 5′UTR of *mrpA* was then ligated to the puromycin resistance marker gene by PCR using primers A and D, information is critical to being better equipped giving the fragment 5′UTR-*puro* with a tail corresponding to the first 25 bases of the 3′UTR of *mrpA*. The marker gene was fused with the 3′UTR of *mrpA*, forming *puro*-3′UTR using primers C and F. The fragment 5′UTR-*puro* was then fused to the *puro*-3′UTR by PCR using primers A and F yielding the recombination cassette 5′UTR-*puro*-3′UTR. 10 μg of the 5′UTR-*puro*-3′UTR linear fragment were transfected by electroporation into *L. infantum* WT to replace both *mrpA* alleles. Recombinants were selected in the presence of 200 μg/mL of puromycin dihydrochloride (Wisent). After 4–5 passages, cells resistant to the drug selection were cloned in SDM-Agar plates (1%), also in the presence of 200 μg/mL puromycin. The *puro/puro* substitution of the *mrpA* gene was confirmed by PCR analysis of the recombinants and Southern blot. Two different PCRs were used: internal PCR was performed using primer set aa' that amplifies a 200-bp *mrpA*-specific region; external PCR was performed using a forward primer located in the *mrpA* 5′ flanking region with a reverse primer in the *mrpA* 3′ flanking region (primer set bb').

2.2.2. mrpA addback and overexpressor mutants

Genes *mrpA* (LinJ.23.0290), *ABCC1* (LinJ.23.0230), *ABCC2* (LinJ.23.0240) and *sat* (LinJ.34.2710) were amplified from *L. infantum* genomic DNA using compatible primer pairs (see Table S1) and PCR fragments were ligated into pGEM T-easy (Promega) to confirm the quality of the insert by standard sequencing. PCR fragments were then cloned in the *Leishmania* expression vector pSP72 *αhygα* (Papadopoulou et al., 1992), which contains the gene hygromycin phosphotransferase (*hyg*), a selectable marker in *Leishmania*. A total of 20 μg of plasmid DNA for episomal expression, either the empty vector (mock) or carrying the genes of interest, were transfected into *L. infantum* WT and $mrpA^{-/-}$ promastigotes by nucleofection, as previously described (Fernandez-Prada et al., 2018). Selection was achieved in the presence of 300 μg/mL hygromycin.

2.3. Mutant selection

Five *L. infantum* puro/puro $mrpA^{-/-}$ Sb-resistant mutants ($mrpA^{-/-}$ CL1 to $mrpA^{-/-}$ CL5) were independently selected from $mrpA^{-/-}$ in 25 cm^2 flasks containing 5 mL SDM-79 medium supplemented with 10% heat inactivated fetal bovine serum (FBS) and 5 μg/mL hemin in the presence of increasing Sb^{III} concentrations. Potassium antimonyl tartrate (Sigma-Aldrich, St Louis, MO, USA) was used as the source of Sb^{III}. The stepwise drug selection ranged from 3 μM up to 180 μM of Sb^{III}. Last-level $mrpA^{-/-}$ Sb-resistant mutants were grown in the absence of drug pressure for 20 passages to revert resistance (rev).

2.4. Drug susceptibility assays

Antileishmanial values in promastigotes were determined by monitoring the growth of parasites after 72 h of incubation at 25 °C in the presence of increasing antimony concentrations, by measuring A_{600} using a Cytation 5 machine (BioTek, USA). EC_{50} against antimony was evaluated in *in vitro* infections using a *luc*-expressing episomal vector (pSP1.2 *luc αhygα*) and PMA-differentiated THP-1 cells as previously described (Fernandez-Prada et al., 2016). Briefly, PMA-differentiated THP-1 macrophages were infected with stationary-phase parasites at a ratio of 18:1, for 2 h at 37 °C in a 5% CO_2 atmosphere. Cells were maintained in drug-free medium for 48 h, after which infected cells were either left untreated or were treated with increasing concentrations of Sb^V (Sodium Stibogluconate, Calbiochem) for 96 h at 37 °C. At this point, THP-1 cells were washed, and luciferase activity was determined using a Cytation 5. Drug-efficacy assays for both promastigotes and macrophage-infecting amastigotes were performed with at least three biological replicates from independent cultures (n = 3). EC_{50} values were calculated based on dose-response curves analysed by non-linear regression with GraphPad Prism 8.0 software (GraphPad Software, La Jolla California, USA). An average of at least three independent biological replicates was performed for each determination. Statistical analyses were performed using unpaired two-tailed t-tests. A p value < 0.05 was considered statistically significant.

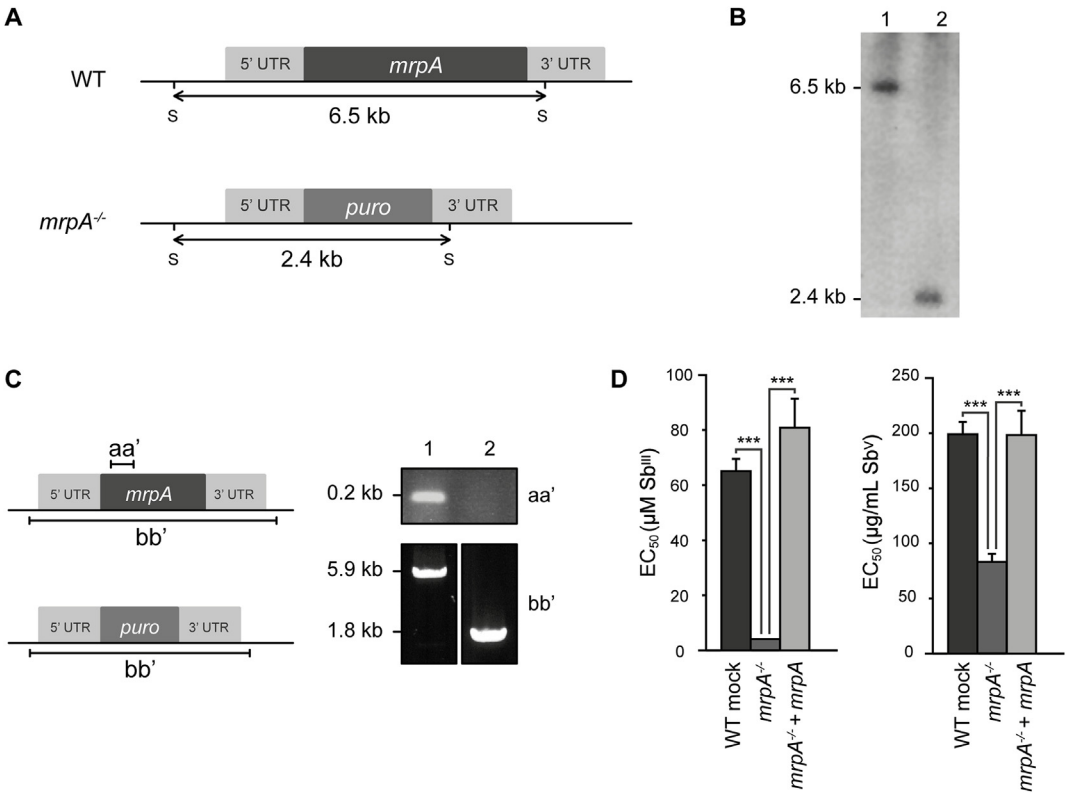

Fig. 1. *mrpA* gene inactivation in *L. infantum*. **(A)** Schematic representation of the *mrpA (LinJ.23.0290)* locus in *L. infantum* before and after integration of the inactivation cassette *PURO*. Relevant *Asc*I restriction sites (S) and size of digested fragments are shown. **(B)** Southern blot analysis with genomic DNAs digested with *Asc*I and probed with [α-^{32}P]-dCTP-labelled 200 bp of 5′ *mrpA L. infantum* coding region. Lane 1, *L. infantum* WT; lane 2, *L. infantum puro/puro mrpA* null mutant; **(C)** PCR analyses (internal and external) for the confirmation of the correct substitution of the *mrpA* gene by the *PURO* cassette. Lane 1, *L. infantum* WT; lane 2, *L. infantum puro/puro mrpA* null mutant; **(D)** Phenotypic evaluation of the *L. infantum mrpA*$^{-/-}$ mutant. EC_{50} values for Sb^{III} and Sb^{V} were determined for the promastigote and amastigote forms of the WT, null mutant and add-back lines. Data are the mean ± SD of three biological replicates. Differences were statistically evaluated by unpaired two-tailed t-test (***$p \leq 0.001$).

2.5. Whole genome sequencing

Genomic DNAs were prepared from a mid-log phase clonal culture of each mutant. Fifty nanograms of purified gDNA were used for paired-end library preparation using Nextera™ DNA Sample preparation kit (Illumina) according to the manufacturer's instructions. The size distribution of Nextera libraries was validated using an Agilent 2100 Bioanalyzer and High Sensitivity DNA chips (Agilent Technologies). Sequencing libraries were quantified with the QuantiFluor® dsDNA System and sequenced using an Illumina HiSeq system at a final concentration of 8 pM. An average genome coverage of over 50-fold was achieved for each *L. infantum mrpA*$^{-/-}$ Sb-resistant mutant. This approach allowed identification of point mutations when compared with the reference genome sequence of *L. infantum* JPCM5 (TriTrypDB version 8.0) (Aslett et al., 2010) and *L. infantum* 263 WT (Ritt et al., 2013). Sequence reads were aligned to the *L. infantum* JPCM5 genome using the software bwa-mem (El Fadili et al., 2009). The maximum number of mismatches was 4, the seed length was 32, and 2 mismatches were allowed within the seed. Read duplicates were marked using Picard (http://broadinstitute.github.io/picard), and GATK was applied for indel realignment and SNP and InDel discovery (McKenna et al., 2010; DePristo et al., 2011) in *L. infantum mrpA*$^{-/-}$ Sb-resistant mutants. PCR amplification and conventional DNA sequencing verified all putative point mutations detected by whole genome sequencing. Copy number variations (CNVs) were derived from read depth coverage by comparing the coverage of uniquely mapped reads between *L. infantum mrpA*$^{-/-}$ Sb-resistant mutants and *L. infantum* 263 WT in small non-overlapping genomic windows (5 kb) for the 36 chromosomes (normalized to the total number of uniquely-mapped reads for each strain) (Chiang et al., 2009). Several python and bash scripts were created to further analyse the data. The sequence data for *L. infantum mrpA*$^{-/-}$ Sb-resistant mutants is available at the NCBI BioProject (https://www.ncbi.nlm.nih.gov/bioproject/) under study accession PRJNA599612 and sample accessions SAMN13762311, SAMN13762312, SAMN13762313, SAMN13762314, SAMN13762315, SAMN13762316, SAMN13762317, SAMN13762318, SAMN13762319, SAMN13762320, corresponding to *mrpA*$^{-/-}$ Sb-resistant CL1 20 ×, CL2 20 ×, CL3 20 ×, CL4 20 ×, CL5 20 ×, CL1 60 ×, CL2 60 ×, CL3 60 ×, CL4 60 × and CL5 60 ×, respectively.

2.6. PFGE and southern blot

Molecular karyotype was obtained from *L. infantum* WT, *mrpA*$^{-/-}$, *mrpA*$^{-/-}$ Sb-resistant mutants, and revertants by separation of chromosomes through pulse field electrophoresis. 10^8 mid-log phase parasites were embedded in low melting point agarose blocks, digested with proteinase K, and electrophoresed in a contour-clamped homogenous electric field apparatus (CHEF Mapper, Bio-Rad, Hercules, CA, USA). The blocks were mounted in 1% agarose gel and electrophoresed in 0.5x Tris-Borate-EDTA running buffer at 5 V cm^{-1} with a 120° separation angle at 14 °C for 30 h. A range of 150–1500 kb was applied for a wide chromosomal separation, resolving most *Leishmania* chromosomes in a single molecular karyotype gel. *Saccharomyces cerevisiae* chromosomes were used as a DNA size marker (Bio-Rad, Hercules, CA, USA). For Southern blots, genomic DNA was isolated using DNAzol reagent (Life Technologies, Carlsbad, CA, USA) following the manufacturer's instructions, then digested with the *Asc*I restriction enzyme (New England Biolabs Inc, Ipswich, MA, USA). Digested genomic DNA or

PFGE-derived molecular karyotype was transferred by capillarity onto nylon membranes (Hybond-N$^+$, Amersham Pharmacia Biotehc, Sunnyvale, CA, USA) and cross-linked with a crosslinker. Blots were hybridized with [α-^{32}P] dCTP-labeled DNA probes according to standard protocol.

3. Results

3.1. *mrpA* is not essential for *L. infantum* survival or infectivity but is key to modulation of parasite antimony sensitivity

The gene coding for the puromycin acetyltransferase (*puro*) was cloned between the 5′- and 3′- *L. infantum mrpA* flanking regions and the linear PURO construct was transfected by electroporation. Instead of using a second selectable marker for substituting the second *mrpA* allele, we decided to explore the possibility of a single round of targeted gene replacement followed by selection for loss of heterozygosity (Gueiros-Filho and Beverley, 1996) by increasing by 2.5 fold the final puromycin-selection pressure. As depicted in Fig. 1A, hybridization with a 5′UTR probe should lead to 6.5 and 2.4 kb *Asc*I-*Asc*I bands in the WT and *puro/puro mrpA*$^{-/-}$ parasites, respectively. As demonstrated in Fig. 1B (lane 2), we were able to generate a homozygous *puro/puro mrpA*$^{-/-}$ line, as no signal for the WT *mrpA* allele at 6.5 kb was detected for the mutant. This result was further confirmed by whole-genome sequencing of the *mrpA*$^{-/-}$ strain, as well as two PCR experiments (Fig. 1C): one targeting 200 bp within the gene (aa') and another targeting the whole *mrpA* ORF using +30 nucleotide external primers (bb'). Once the *mrpA*$^{-/-}$ genotype was confirmed, puromycin-selection was not further continued.

Experimental dose-response assays with the *mrpA*$^{-/-}$ strain revealed an antimony hypersensitive phenotype in both promastigotes (Fig. 1D left panel; 20-fold Sb^{III} EC_{50} shift ($P \leq 0.001$)) and macrophage-infecting amastigotes (Fig. 1D right panel; 2.6-fold Sb^{V} EC_{50} shift ($P \leq 0.001$)). Transfection of the *mrpA* gene as part of an episomal vector in the *mrpA*$^{-/-}$ strain resulted in a complete recovery of the WT phenotype.

3.2. Selection of *mrpA*$^{-/-}$ cells for antimony resistance

Selection of MRPA-independent Sb-resistant mutants began at 1 × EC_{50} value for the *mrpA*$^{-/-}$ strain (3.2 μM) up to 60 × IC_{50} (180 μM), which is approximately 2.5-fold the EC_{50} of the WT parental line. The selection procedure was fast (3 subsequent passages per drug concentration), and cells rapidly adapted to growing concentrations of Sb. All five clones reached the final selection step at 60 × EC_{50}. In order to follow the evolution of the resistant phenotype for each clone, dose-response assays were conducted at passage 3 (P3) for 1 × , 4 × , 10 × , 20 × and 60 × EC_{50} selection steps. As depicted in Fig. 2, all five clones reached similar EC_{50} values at selection step P3 10 × EC_{50}, with clones CL1 and CL2 displaying slightly higher values (23 and 20 μM, respectively). While these two clones showed a great increase in EC_{50} values at selection step P3 20 × EC_{50} (48 and 63 μM, respectively), clones CL3, CL4 and CL5 remained with values around 20 μM. Once the final selection step was reached (P3 60 × EC_{50}), clones were reevaluated for sensitivity against antimony. Clones CL1 and CL2 demonstrated the highest EC_{50} values (105 and 141 μM), higher than the EC_{50} value for the parental WT strain (approximately 65 μM). The other clones reached modest but significant increases in their EC_{50} values (CL3: 35; CL4: 48; and CL5: 38 μM), which represent a 6-fold mean increase compared to the unselected parental *mrpA*$^{-/-}$ strain. Potentially different mechanisms of adaptation to Sb are being deployed by independent clones.

3.3. Exposure of *mrpA*$^{-/-}$ mutants to increasing concentrations of Sb results in major changes in CNVs

Whole-genome sequencing was conducted by Illumina next-generation sequencing on the five independent *L. infantum mrpA*$^{-/-}$ Sb-resistant lines selected at 20 × and 60 × EC_{50}, as well as the isogenic *L. infantum* WT line. For all strains, this produced genome assemblies of 31 Mb with a coverage depth of at least 50-fold.

Several cases of supernumerary chromosomes were observed in the *mrpA*$^{-/-}$ Sb-resistant mutants (Fig. 3 and Dataset S1), the majority of which had $\log_2$ *mrpA*$^{-/-}$ Sb-resistant/WT read ratios close to 0.5. Parasites from the *Leishmania Leishmania* subgenus have predominantly disomic genomes, and this should thus represent a gain of one allele compared to WT parasites (going from 2 to 3 chromosome copies). Most supernumerary chromosomes were shared by the mutants; chromosomes 6 and 9 were consistently increased in all *mrpA*$^{-/-}$ Sb-resistant mutants except CL4, chromosomes 18 (except in CL5 at 60 ×) and 23 were increased in all five mutants. Markedly, chromosome 23 passed from disomic to tetrasomic for CL5. Chromosome 8 was increased for clones CL1, CL3 and CL4; and chromosome 11 for clones CL1, CL4 and CL5. Finally, CL1, CL2 and CL4 gained a copy of chromosome 12, thus becoming pentasomic. There were no major differences between genome sequences at 20 × and 60 × , with the exception of several chromosome losses, which were consistent with the loss of one allele (Fig. 3, Dataset S1). These losses affected chromosome 31 in CL2, CL3 and CL5. Overall, CL3 was the most divergent clone and displayed the highest level of chromosome-level CNVs compared to the four other mutants (Fig. 3). However, this did not correlate with reduced Sb sensitivity.

Normalized read depth coverage allowed the identification of amplified and deleted genomic loci in the *mrpA*$^{-/-}$ Sb-resistant mutants. These are characterized by punctuated series of adjacent genomic windows whose normalized read coverage varies compared to the WT baseline, as observed for chromosome 23 in more than one mutant (Dataset S2). In fact, for chromosome 23, the amplified region was large, covering 110 kb and 75 kb in mutants CL2 and CL5, respectively (Fig. 4A and B). This amplification starts at one subtelomeric end and encompasses the region where the *mrpA* gene was located before generation of the null mutant. This subtelomeric amplification was suspected to be a linear amplicon rather than an intrachromosomal tandem duplication due to its length, its location close to a telomere, and the increase in number of normalized reads. Beside the amplification, normalized read depth coverage was higher in the mutant for the entire length of the chromosome (Fig. 4B) and supported the increase in ploidy described above for chromosome 23 (Fig. 3). Markedly, while the change of ploidy for all five clones seems to have been achieved at 20 × (Fig. 4A), the 60 × selection step was required to induce the subtelomeric amplification observed for clones CL2 and CL5 (Fig. 4B). Hybridization of chromosomes separated by PFGE with probe-targeting gene LinJ.23.0220 (located nearby *mrpA* on chromosome 23) supported the NGS data and confirmed that two mutants had linear amplifications corresponding to the subtelomeric region of the chromosome (Fig. 4C, lanes 4 and 7). Regarding clone CL1, normalized read depth coverage of chromosome 23 revealed 2 peaks, which are also comprised in the subtelomeric amplifications observed for CL2 and CL5 (Fig. 4B). The first corresponds to the genomic region LinJ.23:65000-80000, which contains the partial ORF of LinJ.23.0230 (ABCC1) and the complete sequence of LinJ.23.0240 (ABCC2) (see chromosme 23 in Dataset S2); the second corresponds to *mrpA* gene-flanking regions, an artifact due to a duplication of the puro selectable marker within the 5′ and 3' UTRs of *mrpA*.

3.4. Link between gene amplification and drug resistance

To verify if linear DNA amplifications were reversible, CL2 and CL5 (as well as the other clones) were subcultured in the absence of Sb

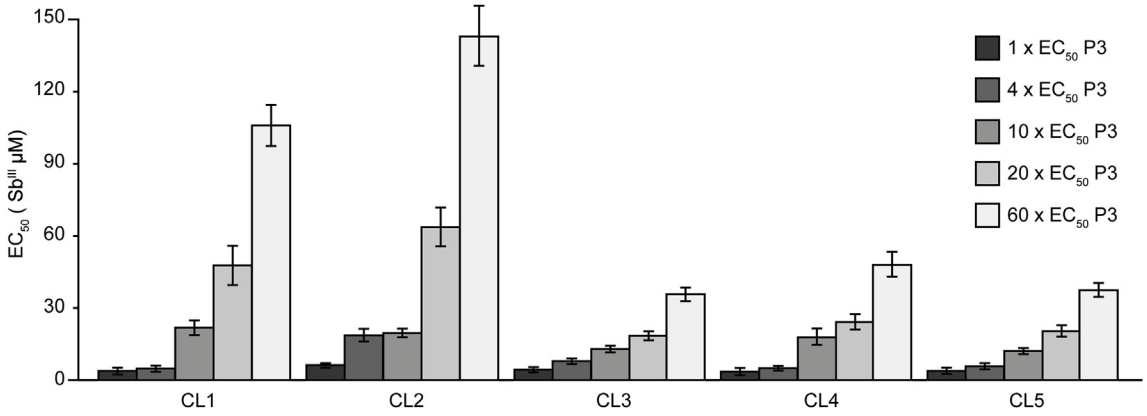

Fig. 2. Phenotypic appraisal of the *mrpA*$^{-/-}$ clones submitted to stepwise selection for antimony resistance. EC_{50} values in promastigotes of the different *L. infantum mrpA*$^{-/-}$ mutants at P3 for 1 ×, 4 ×, 10 ×, 20 × and 60 × EC_{50} selection steps were determined by monitoring the growth of parasites after 72-h of incubation at 25 °C in the presence of increasing antimony concentrations, by measuring A_{600} using a Cytation 5 (BioTek, USA). Data are the mean ± SD of three biological replicates.

pressure for 20 passages. The chromosomes of the revertants of CL2 and CL5 were separated by PFGE with a probe targeting the gene LinJ.23.0220. Both clones lost their respective linear amplicon after 20 passages in the absence of Sb pressure (lanes 5 and 8 of Fig. 4C).

Next, the potential resensitization of clones after 20 passages in the absence of Sb pressure was evaluated phenotypically. As depicted in Fig. 4D, the EC_{50} values for all five clones were significantly reduced compared with their *mrpA*$^{-/-}$ Sb-resistant counterparts. CL1 and CL2 showed the greatest shift in EC_{50} values with 3- and 5-fold decreases, respectively. Shifts for clones CL3, CL4 and CL5 were more modest but still significant. None of the revertants reached the levels of hypersensitivity demonstrated by the parental *mrpA*$^{-/-}$ strain before stepwise selection.

We looked for genes that were both part of the linear amplicons identified in clones CL2 and CL5, and were present in the genomic region enriched in CL1 (LinJ.23:65000-80000), and noticed the presence of *ABCC1* and *ABCC2* genes (Leprohon et al., 2006). Overexpression of *ABCC1 and ABCC2* was performed by stable episomal transfection in the *mrpA*$^{-/-}$ background, but also in WT parasites (Fig. 5A). While ABCC1 did not yield a resistant phenotype, overexpression of ABCC2 caused a 2-fold reduction in Sb sensitivity in the *mrpA*$^{-/-}$ strain. No effect was observed in the WT background for either ABCC1 or ABCC2 (Fig. 5A).

3.5. Point mutations and role of a serine acetyltransferase in antimony resistance

A search for point mutations revealed very few homozygous SNPs in any of the five *mrpA*$^{-/-}$ Sb-resistant mutants (Dataset S3), and none within any known drug resistance-related ORF. Homozygous SNPs were located in genes coding for hypothetical proteins, with the exception of LinJ.35.0500, which codes for a large proteophosphoglycan protein often found mutated in our various sequencing screens. Genes coding for hypothetical proteins were not studied further, as there was no recurrence among mutants for these genes. Heterozygous SNPs were more frequent, so they were clustered according to the number of clones carrying mutations in the same ORF (Supplementary Figs. S1 and S2; Dataset S3). Eight heterozygous SNPs were common to the 5 clones at both 20 × and 60 ×. In all cases, exactly the same mutation was present. Given the high probability that our laboratory strain already carries these SNPs (absent in the reference strain), they were not further analysed. No SNPs were found by NGS in the *aqp1* gene, which, when mutated or deleted, leads to a reduction in antimony uptake by the parasite (Monte-Neto et al., 2015). This was further confirmed by targeted PCR and sequencing of the *aqp1* ORF from all five clones at both 20 × and 60 × selection steps. In order to find potential SNP candidates, the different clones were examined for SNPs occurring in the same ORF but at different positions. Only one SNP located in gene LinJ.34.2710 (serine acetyltransferase *sat* gene) in clones CL1, CL2 and CL4 at the 60 × selection step fulfilled this requirement (Supplementary Fig. S2). The mutations identified in the three *mrpA*$^{-/-}$ Sb-resistant mutants by NGS and confirmed by targeted PCR were *sat*^{Q390K} for CL1, *sat*^{G321R} for CL2 and *sat*^{G325R} for CL4. Interestingly, the heterozygous SNPs in the *sat* ORF for CL1, CL2 and CL4 were lost from the populations of the clones when grown for 20 passages in the absence of antimony.

We overexpressed the three *sat* heterozygous mutations (as well as the WT version of the gene) in both *mrpA*$^{-/-}$ (Fig. 5B) and WT backgrounds (Fig. 5C). Overexpression of the *sat*^{WT} copy did not confer further Sb resistance in the *mrpA*$^{-/-}$ strain nor in the WT cell line. However, overexpression of all three mutated variants of the *sat* gene resulted in a significant decrease in Sb sensitivity in the *mrpA*$^{-/-}$ strain: *sat*^{Q390K} (2.12-fold), *sat*^{G321R} (2.94-fold) and *sat*^{G325R} (3.23-fold). That said, only two of these three mutations, *sat*^{G321R} and *sat*^{G325R}, had a significant effect on Sb susceptibility in the WT strain (1.62- and 1.99-fold, respectively).

4. Discussion

Although the mode of action of Sb remains unclear, several mechanisms of drug resistance have been extensively described in *Leishmania* parasites, including modulation of Sb detoxification pathways (Mukherjee et al., 2007; Wyllie et al., 2004), altered drug internalization (Monte-Neto et al., 2015; Marquis et al., 2005), and increased efflux (Mukhopadhyay et al., 1996). However, the most frequently reported mechanism of Sb resistance is the intracellular sequestration of Sb-thiol conjugates, mediated by ABC-transporter MRPA (Gazanion et al., 2016; Ouellette and Papadopoulou, 1993; Leprohon et al., 2015; Ponte-Sucre et al., 2017). In this study, in order to search for MRPA-independent mechanisms of drug resistance against Sb, we utilized a unique combination of targeted disruption of the *mrpA* gene, stepwise drug-resistance selection, and next-generation sequencing (NGS) in *L. infantum* parasites.

Firstly, we demonstrated that MRPA is not essential for the survival and infectivity of *L. infantum in vitro*. As suspected, sensitivity to Sb was greatly increased in the *mrpA*$^{-/-}$ mutant. MRPA-deficient promastigotes demonstrated a 20-fold decrease in their EC_{50} value against Sb^{III}. That said, *mrpA*$^{-/-}$ amastigotes showed a modest 2.6-fold increase in sensitivity against Sb^{V}. Of note, although *mrpA* is frequently found in promastigote drug screens, and validated as a drug resistance gene with

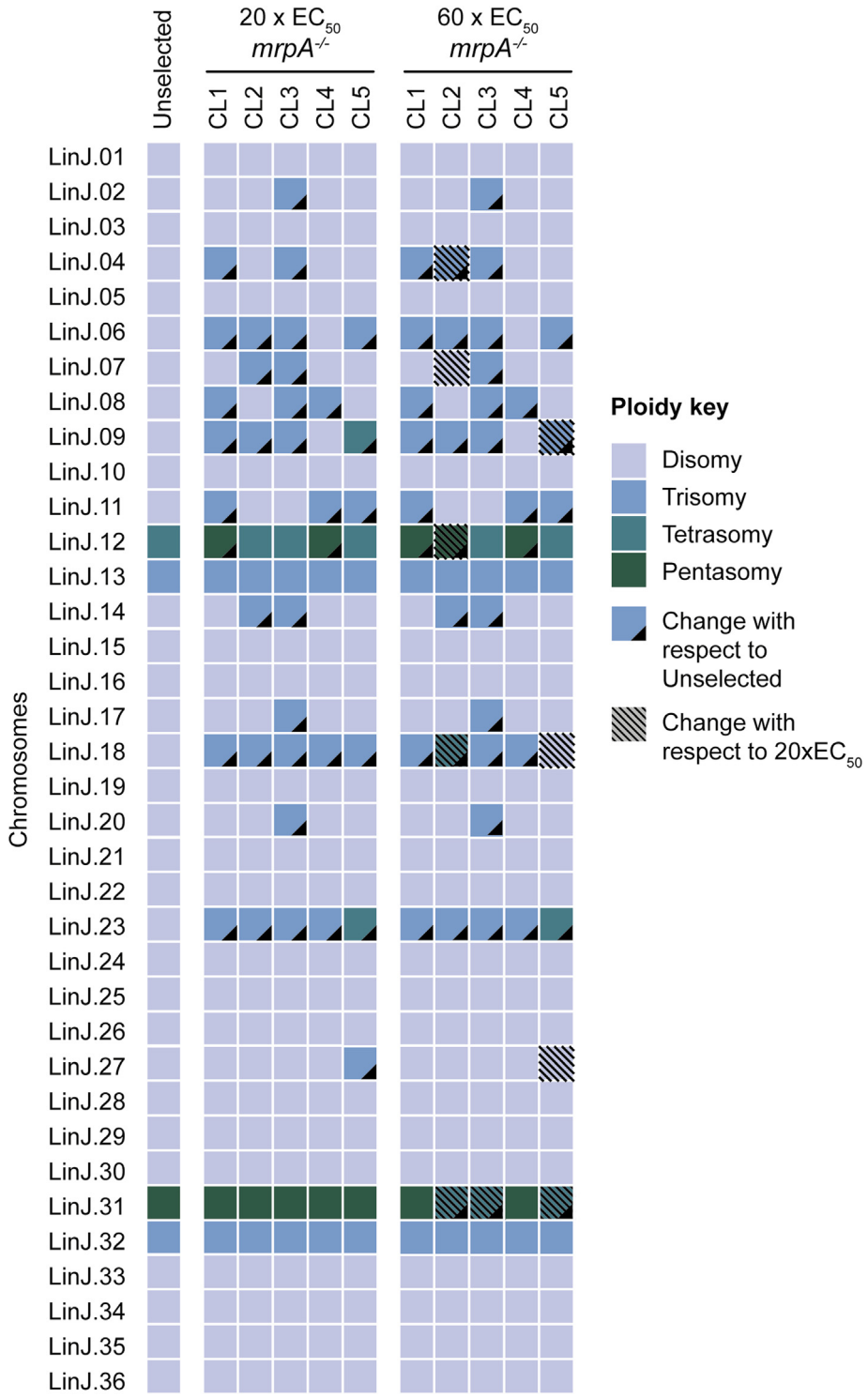

Fig. 3. Dynamics of aneuploidy of *L. infantum mrpA*$^{-/-}$ during *in vitro* adaptation to antimony. Heatmap representation of $\log_2$-transformed normalized Sb-resistant/unselected read ratio for all 36 chromosomes in the five independent *L. infantum mrpA*$^{-/-}$ Sb-resistant lines selected at 20 × and 60 × EC_{50}. Chromosomes were divided into non-overlapping 5 kb genomic windows and median *L. infantum mrpA*$^{-/-}$ Sb-resistant/unselected reads ratios for each chromosome were normalized according to the total number of reads followed by $\log_2$-transformation (See Dataset S1 for further details).

intracellular parasites (El Fadili et al., 2005), its role as an *in vivo* marker of Sb resistance is controversial since it's not always found to be amplified in drug-resistant clinical isolates (Mukherjee et al., 2007; Moreira et al., 1998; Barrera et al., 2017) but increased in *mrpA* CNVs was found to be the main driver of molecular preadaptation to antimony resistance in *L. donovani* (Dumetz et al., 2018). Interestingly, two different gain-of-function screens using genomic overexpression libraries coupled to NGS (Cos-Seq) revealed a very pronounced enrichment of the *mrpA* gene in promastigotes progressively exposed to Sb^{III}, but not in macrophage-infecting amastigotes exposed to Sb^{V} (Gazanion et al., 2016; Fernandez-Prada et al., 2018), showing that MRPA-independent Sb-resistance mechanisms can be deployed by the parasite.

In order to identify novel MRPA-independent Sb-resistance

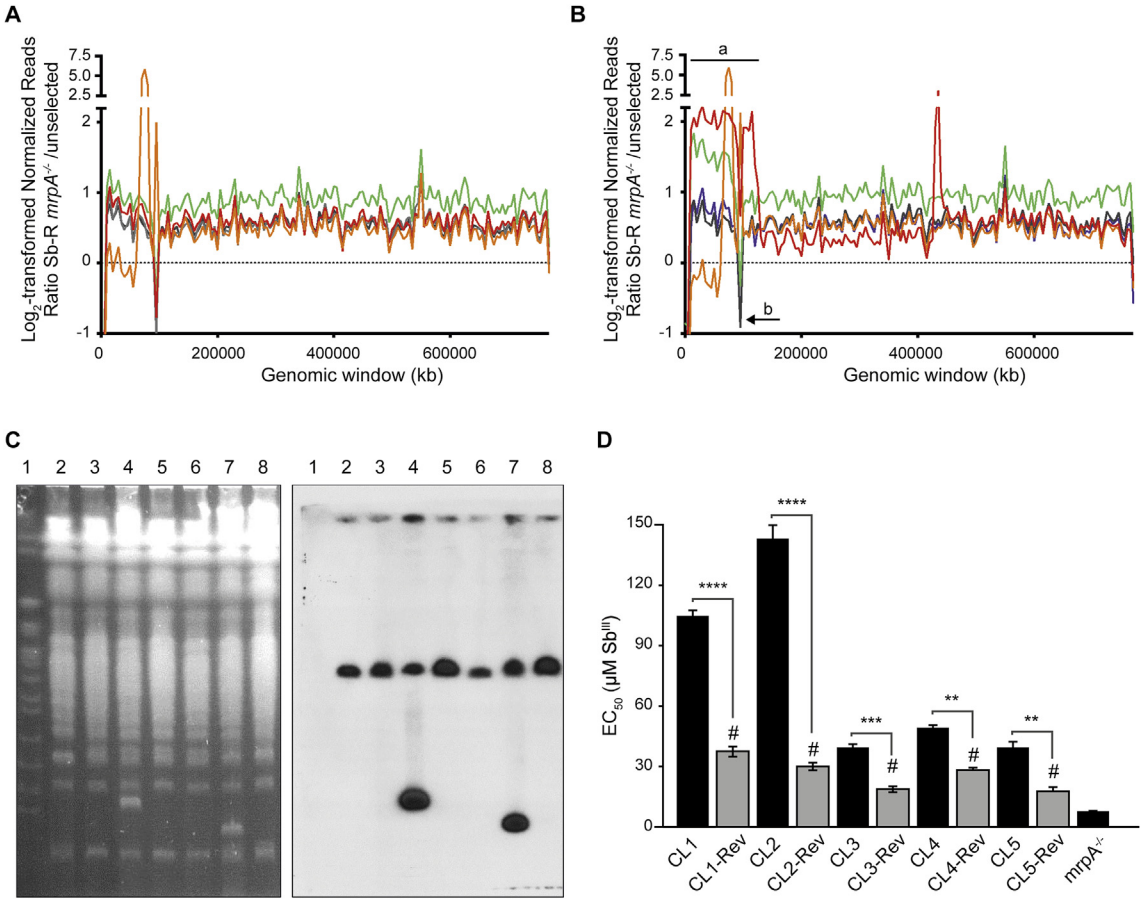

Fig. 4. Extrachromosomal amplifications in *L. infantum mrpA*$^{-/-}$ Sb-resistant mutants and phenotypic evaluation of the revertant strains. (A) Log_2-transformed 20 × Sb-resistant mutants/unselected reads ratios for non-overlapping 5 kb genomic windows on chromosome 23. Orange, CL1; Red, CL2; Grey, CL3; Purple, CL4; and Green, CL5. **(B)** Log_2-transformed 60 × Sb-resistant mutants/unselected reads ratios for non-overlapping 5 kb genomic windows on chromosome 23. Orange, CL1; Red, CL2; Grey, CL3; Purple, CL4; and Green, CL5. *a*, amplified region in clones CL2 and CL5; *b*, gap in the sequencing reads resulting from the deletion of the *mrpA* gene. **(C)** Chromosomes were separated by PFGE and hybridized with a probe targeting gene LinJ.23.0220. Lanes: 1, molecular weight marker; 2, *L. infantum* WT; 3, unselected *L. infantum mrpA*$^{-/-}$ CL2; 4, 60 × Sb-resistant CL2; 5, revertant CL2; 6, unselected *L. infantum mrpA*$^{-/-}$ CL5; 7, 60 × Sb-resistant CL5; 8, revertant CL5. **(D)** EC_{50} values for Sb^{III} were determined for the promastigote forms of *L. infantum mrpA*$^{-/-}$ Sb-resistant clones and their revertant (Passage 20 in absence of Sb pressure) counterpart lines by monitoring the growth of parasites after 72-h of incubation at 25 °C in the presence of increasing antimony concentrations, by measuring A_{600} using a Cytation 5 (BioTek, USA). Data are the mean ± SD of three biological replicates. Differences were statistically evaluated by unpaired two-tailed t-test (*$p \leq 0.01$, ***$p \leq 0.001$; ****$p \leq 0.0001$ between each *mrpA*$^{-/-}$ Sb-resistant mutant and its derived revertant line; and $^{\#}p \leq 0.05$ between each revertant and the unselected *mrpA*$^{-/-}$ parental cell line). (For interpretation of the references to color in this figure legend, the reader is referred to the Web version of this article.)

mechanisms, we evaluated the ability of five independent *L. infantum mrpA*$^{-/-}$ clones to become resistant to Sb^{III}. In this study, all five clones were able to significantly decrease their sensitivity to Sb in comparison to the parental *L. infantum mrpA*$^{-/-}$ line, but only two clones (CL1 and CL2) were able to surpass the EC_{50} value calculated for the parental WT strain. These results point to different genomic adaptation mechanisms occurring in each of the five independent clones. As gene expression in *Leishmania* is regulated predominantly by gene dosage (Leprohon et al., 2015; Iantorno et al., 2017), we proceeded to identify CNVs and SNP events in the five clones at two different selection steps, 20 × and 60 × EC_{50} of the unselected *L. infantum mrpA*$^{-/-}$ strain, by NGS (Leprohon et al., 2015). Normalized read depth coverage identified several chromosomes in the *mrpA*$^{-/-}$ Sb-resistant clones whose ploidy was altered compared to the unselected parental line. However, no common pattern among karyotypes was found (except for chromosomes 18, 23 and 31, which displayed common changes in CNVs for almost all the clones), which makes it difficult to establish a link between phenotypes and karyotype variations. This is not new as *Leishmania* chromosome ploidy in individual parasites is known to vary rapidly in response to changing environments, including routine cell culture, resulting in mosaic aneuploidy (Sterkers et al., 2011; Ubeda et al., 2008). A recent study identified major changes in chromosomal somy, gene expression and gene dosage driven by Sb^{III} in *L. braziliensis* (Patino et al., 2019). Markedly, our results for chromosomes 4 (CL1 and CL3), 11 (CL1, CL4 and CL5), 14 (CL2 and CL3) and 23 (all the clones) are in line with those reported by Patino and co-workers (Patino et al., 2019).

Leishmania accumulates Sb^{III} primarily through aquaglyceroporin AQP1, which is involved in volume regulation and osmotaxis (Gourbal et al., 2004). Loss-of-function mutations in its ORF, as well as CNVs at the level of the subtelomeric region of chromosome 31 harboring the *aqp1* gene result in decreased Sb^{III} susceptibility (Monte-Neto et al., 2015; Mukhopadhyay et al., 2011; Plourde et al., 2015; Imamura et al., 2016). Sb-selection did not induce mutations in the *aqp1* gene in any of our *mrpA*$^{-/-}$ Sb-resistant clones. However, CL2, CL3, and CL5 reduced the ploidy of chromosome 31 by one copy at 60 × EC_{50}, which could result in decreased Sb uptake. This finding corroborates previous studies demonstrating that *Leishmania* parasites submitted to experimental Sb selection rely on aneuploidy as their first adaptation mechanism, even before emergence and eventual fixation of SNPs (Mukherjee et al., 2013; Monte-Neto et al., 2015; do Monte-Neto et al., 2011).

Alternatively, chromosome 23, harboring the H locus in which *mrpA*

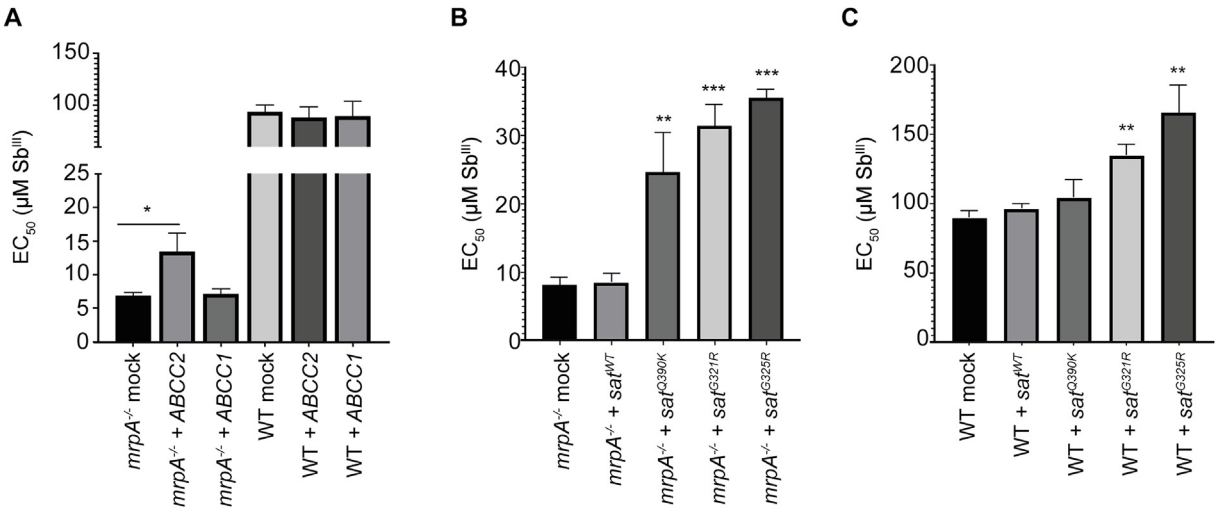

Fig. 5. Functional analysis of ABCC1/ABCC2 overexpression and different mutations in the *sat* gene in Sb susceptibility. (A) Impact of overexpression of the genes ABCC1 and ABCC2 on the Sb-sensitivity profile of both WT and *mrpA*$^{-/-}$ lines. **(B)** Impact of overexpression of the *sat* gene, as well as three mutated versions, on the Sb-sensitivity profile of *mrpA*$^{-/-}$ parasites. **(C)** Impact of overexpression of the *sat* gene and its three mutated versions on the Sb-sensitivity profile of WT parasites. Data are the mean ± SD of three biological replicates. Differences were statistically evaluated by unpaired two-tailed t-test (∗$p \leq 0.05$, ∗∗$p \leq 0.01$, ∗∗∗$p \leq 0.001$).

is located (Leprohon et al., 2009a), was amplified in all five of our *mrpA*$^{-/-}$ Sb-resistant clones, transitioning from a disomic to trisomic ploidy in CL1 to 4, and to a tetrasomic ploidy in CL5. Markedly, the subtelomeric region of chromosome 23 was further amplified in CL2 and CL5 in the form of two different linear amplicons. On the other hand, CL1 demonstrated major enrichment of a 15-kb genomic region comprising the partial sequence of LinJ.23.0230 (*ABCC1*) and the complete ORF of LinJ.23.0240 (*ABCC2*), which is also included in the linear amplicons detected for CL2 and CL5. While it has been shown that *mrpA* is the only gene within the H locus that contributes to Sb resistance when overexpressed (Dumetz et al., 2018; Leprohon et al., 2009b; Callahan and Beverley, 1991), we decided to evaluate the impact of ABCC1 and ABCC2 in the *mrpA*$^{-/-}$ background. Overexpression of ABCC2 resulted in a 2-fold increase in *mrpA*$^{-/-}$ tolerance to Sb; an alteration not seen in the WT. ABCC2 is part of the ABCC subfamily, a class of proteins known to be involved in detoxification of metals in *Leishmania* (Légaré et al., 2001; Leprohon et al., 2009b). In wild-type cells only the transfection of the ABCC family member MRPA (ABCC3) produces Sb resistance. However in *L. tarentolae* revertant cells with unknown factors contributing to resistance, ABCC4 and 5 were shown to produce resistance as well (Leprohon et al., 2009b). Here when MRPA is absent, cells become hypersensitive to Sb, and in this case we were able to show that ABCC2 contributes to resistance in this specific cellular context.

Amplicons generated from the H locus containing *mrpA* have previously been found to be unstable in the absence of Sb pressure (Leprohon et al., 2009a, 2015). Likewise, in our experiment, after 20 passages in the absence of Sb drug pressure, both CL2 and CL5 lost their respective linear amplicons and significantly reduced their tolerance to Sb. However, they did not fully recover the *mrpA*$^{-/-}$ phenotype, suggesting that other mutations contribute to resistance. Indeed, our screen for potential SNPs involved in the Sb-resistant *mrpA*$^{-/-}$ phenotype lead to the identification of three different heterozygous mutations (Q390K, G321R and G325R) in gene LinJ.34.2710 at 60 × EC_{50}, each one in a different *mrpA*$^{-/-}$ Sb-resistant clone. The gene LinJ.34.2710 encodes a serine acetyltransferase (SAT) which has recently been surmised to be involved in the two routes of *de novo* cysteine synthesis in *Leishmania* (Marciano et al., 2010). *L*-serine is conjugated with acetyl-CoA by SAT to form the intermediate product *O*-acetylserine, which is then converted to *L*-cysteine by cysteine synthase (CS). Cysteine is the precursor moiety for biosynthesis of GSH and trypanothione, which are the main cellular defense mechanisms against oxidative stress, involved in Sb detoxification (Grondin et al., 1997; Haimeur et al., 2000; Papadopoulou et al., 1996; Singh et al., 2016). Our three clones displaying a mutation in the *sat* gene were also those exhibiting the highest EC_{50} against Sb after reaching the last step of selection (Fig. 2). These heterozygous SNPs were not fixed in the genome of the parasite as they disappeared, probably by allelic exchange, after 20 passages in the absence of Sb drug pressure, which also led to a great decrease in Sb tolerance of the revertant clones. Most likely cells in the population with a mutated *sat* were at a disadvantage when grown in the absence of Sb^{III}. Likewise, in a clinical context, most of the known Sb-resistant mechanisms relying on CNVs and heterozygous mutations are reverted without drug pressure. However, reversion has not been achieved in the Indian subcontinent, where Sb-resistant *Leishmania* parasites remain highly prevalent despite discontinuing the use of Sb as first-line treatment. Imamura and co-workers identified a 2-nt insertion in the *aqp1* gene in 52 strains isolated from antimonial treatment failure patients (Imamura et al., 2016). Its dissemination could have been favored, even in the absence of Sb-based treatments, by an increased fitness of Sb-resistant parasites (Dumetz et al., 2018; Vanaerschot et al., 2013) and cross-selection through chronic exposure to arsenic-contaminated water (Perry et al., 2011, 2013). In our case, we were not able to achieve a full recovery of the *mrpA*$^{-/-}$ sensitive phenotype after 20 passages in absence of Sb^{III}. This could be caused by different metabolic adaptations acquired during the selection process (*e.g.* changes in mitochondrial metabolism or in membrane fluidity (Berg et al., 2013)) that would require extended subculturing to be diluted in the resensitized population.

Our preferred method for studying the role of SAT mutations was episomal transfection of wild-type and mutated forms of the gene in the *mrpA*$^{-/-}$ mutant and WT. All three mutations conferred resistance to the *mrpA*$^{-/-}$, but only the two with the strongest phenotype induced a significant shift in EC_{50} value against Sb in the WT. Of note, all three mutations occurred within the predicted CoA binding site (cysE domain) of the protein (aa 224–390). SAT mutations may be leading to more efficient production of *O*-acetylserine or to more stable CS and SAT protein complex formation. In either case, the SAT/CS complex would be capable of providing more than the necessary amount of cysteine for biosynthesis of GSH, and thus trypanothione, which can bind to Sb to facilitate its elimination – as well as counteract ROS formation (Singh et al., 2016). Since SAT mutations could increase thiols (*e.g.*

trypanothione and glutathione) through, by example, disabling of a regulatory site or negative feedback loop limiting such products, future work should evaluate the content of the different thiol species in the *mrpA*$^{-/-}$ mutant background as well as in the Sb-resistant *mrpA*$^{-/-}$ clones and establish whether this correlates with specific changes in sensitivity to Sb^{III}.

Amplification of MRPA or loss-of-function mutations in AQP1 are the primary mechanisms of Sb resistance in both laboratory and field isolates (Mukherjee et al., 2007; Dumetz et al., 2018; Imamura et al., 2016). That said, these strong traits could preclude the identification of secondary mechanisms/markers of drug resistance against Sb. In oder to evaluate the occurrence of SNPs in the *sat* gene in clinical isolates, the TritrypDB database (Aslett et al., 2010) was mined for genetic variations in the *sat* gene among its *L. donovani* datasets, which comprise a total of 252 isolates. Six non-synonymous polymorphisms were found (lines 234,631 to 264,639 highlighted in yellow in the Ldono_allTritryp_SNPs tab of Dataset 4). The strains harboring the changes were retrieved from a nucleotide alignment of the *sat* gene for the 252 isolates (tab strains of Dataset 4). Most of the strains including SNPs in the *sat* gene are associated with a dataset derived from a study of Ethiopian *L. donovani* (Zackay et al., 2018). However, Zackay and co-workers only explored the drug-resistant profile of these strains against methotrexate because they were able to identify CNVs for the folate transporter in most of the Northeast strains (Zackay et al., 2018). On the other hand, some strains with polymorphism in the *sat* gene are part of the Indian-sucbontinent cluster 1 (ISC1) identified by Imamura and co-workers (Imamura et al., 2016). Intriguingly, intra-chromosomal amplification of *mrpA* was present in all core population isolates but was absent in ISC1. It would be interesting to address whether the presence of mutations in the *sat* gene in the absence of duplication of *mrpA* is affecting the sensitivity of ISC1 strains. Additional work may indicate whether these mutations in the *sat* gene are directly related to Sb selection, and treatment failure, or simply provide a general fitness gain that allows the parasite to survive in stressful conditions.

5. Conclusion

In this study, we combined targeted gene disruption, stepwise drug-resistance selection, and NGS in *L. infantum* to search for novel Sb-resistance mechanisms deployed by the parasite when ABC transporter MRPA is abolished. We demonstrated that MRPA is not essential for survival of *Leishmania*, and its disruption does not impair the parasite's infectivity. Furthermore, we revealed major changes in the karyotype and CNVs of the subtelomeric region of chromosome 23 in our five *mrpA* null mutants exposed to increasing concentrations of Sb. Our results reinforce and expand knowledge on the complex nature of Sb resistance in *Leishmania* by highlighting two previously unreported Sb-resistance related genes, *sat* and *ABCC2*, which are putatively linked to thiol biosynthesis and transport in these parasites. These findings could have a significant positive impact on the control of this critical zoonotic disease.

Declaration of competing interest

The authors declare that they have no known competing financial interests or personal relationships that could have appeared to influence the work reported in this paper.

Acknowledgements

This work was supported by a Natural Sciences and Engineering Research Council of Canada Discovery Grant RGPIN-2017-04480 and by the Canada foundation for Innovation (www.innovation.ca), grant number 37324; both awarded to CFP. Work in the MO lab is supported by a CIHR Foundation Grant. MO holds a Canada Research Chair. N.D. is supported by *Fonds de recherche du Québec – Nature et technologies* (FRQNT) scholarship program.

Appendix A. Supplementary data

Supplementary data to this article can be found online at https://doi.org/10.1016/j.ijpddr.2020.03.003.

References

Abranches, P., Silva-Pereira, M.C., Conceicao-Silva, F.M., Santos-Gomes, G.M., Janz, J.G., 1991. Canine leishmaniasis: pathological and ecological factors influencing transmission of infection. J. Parasitol. 77 (4), 557–561.

Aslett, M., Aurrecoechea, C., Berriman, M., Brestelli, J., Brunk, B.P., Carrington, M., et al., 2010. TriTrypDB: a functional genomic resource for the Trypanosomatidae. Nucleic Acids Res. 38 (Database issue), D457–D462.

Barrera, M.C., Rojas, L.J., Weiss, A., Fernandez, O., McMahon-Pratt, D., Saravia, N.G., et al., 2017. Profiling gene expression of antimony response genes in *Leishmania (Viannia) panamensis* and infected macrophages and its relationship with drug susceptibility. Acta Trop. 176, 355–363.

Berg, M., Vanaerschot, M., Jankevics, A., Cuypers, B., Maes, I., Mukherjee, S., et al., 2013. Metabolic adaptations of *Leishmania donovani* in relation to differentiation, drug resistance, and drug pressure. Mol. Microbiol. 90 (2), 428–442.

Callahan, H.L., Beverley, S.M., 1991. Heavy metal resistance: a new role for P-glycoproteins in *Leishmania*. J. Biol. Chem. 266 (28), 18427–18430.

Chiang, D.Y., Getz, G., Jaffe, D.B., O'Kelly, M.J., Zhao, X., Carter, S.L., et al., 2009. High-resolution mapping of copy-number alterations with massively parallel sequencing. Nat. Methods 6 (1), 99–103.

DePristo, M.A., Banks, E., Poplin, R., Garimella, K.V., Maguire, J.R., Hartl, C., et al., 2011. A framework for variation discovery and genotyping using next-generation DNA sequencing data. Nat. Genet. 43 (5), 491–498.

Dey, S., Ouellette, M., Lightbody, J., Papadopoulou, B., Rosen, B.P., 1996. An ATP-dependent As(III)-glutathione transport system in membrane vesicles of *Leishmania tarentolae*. Proc. Natl. Acad. Sci. U. S. A. 93 (5), 2192–2197.

Dumetz, F., Cuypers, B., Imamura, H., Zander, D., D'Haenens, E., Maes, I., et al., 2018. Molecular preadaptation to antimony resistance in *Leishmania donovani* on the Indian subcontinent. mSphere 3 (2).

El Fadili, K., Messier, N., Leprohon, P., Roy, G., Guimond, C., Trudel, N., et al., 2005. Role of the ABC transporter MRPA (PGPA) in antimony resistance in *Leishmania infantum* axenic and intracellular amastigotes. Antimicrob. Agents Chemother. 49 (5), 1988–1993.

El Fadili, K., Drummelsmith, J., Roy, G., Jardim, A., Ouellette, M., 2009. Down regulation of KMP-11 in *Leishmania infantum* axenic antimony resistant amastigotes as revealed by a proteomic screen. Exp. Parasitol. 123 (1), 51–57.

Fernandez-Prada, C., Vincent, I.M., Brotherton, M.C., Roberts, M., Roy, G., Rivas, L., et al., 2016. Different mutations in a P-type ATPase transporter in *Leishmania* parasites are associated with cross-resistance to two leading drugs by distinct mechanisms. PLoS Neglected Trop. Dis. 10 (12), e0005171.

Fernandez-Prada, C., Sharma, M., Plourde, M., Bresson, E., Roy, G., Leprohon, P., et al., 2018. High-throughput Cos-Seq screen with intracellular *Leishmania infantum* for the discovery of novel drug-resistance mechanisms. Int. J. Parasitol.: Drugs Drug Resistance 8 (2), 165–173.

Gazanion, E., Fernandez-Prada, C., Papadopoulou, B., Leprohon, P., Ouellette, M., 2016. Cos-Seq for high-throughput identification of drug target and resistance mechanisms in the protozoan parasite *Leishmania*. Proc. Natl. Acad. Sci. U. S. A. 113 (21), E3012–E3021.

Gourbal, B., Sonuc, N., Bhattacharjee, H., Legare, D., Sundar, S., Ouellette, M., et al., 2004. Drug uptake and modulation of drug resistance in *Leishmania* by an aquaglyceroporin. J. Biol. Chem. 279 (30), 31010–31017.

Grondin, K., Haimeur, A., Mukhopadhyay, R., Rosen, B.P., Ouellette, M., 1997. Co-amplification of the gamma-glutamylcysteine synthetase gene gsh1 and of the ABC transporter gene pgpA in arsenite-resistant *Leishmania tarentolae*. EMBO J. 16 (11), 3057–3065.

Gueiros-Filho, F.J., Beverley, S.M., 1996. Selection against the dihydrofolate reductase-thymidylate synthase (DHFR-TS) locus as a probe of genetic alterations in *Leishmania major*. Mol. Cell Biol. 16 (10), 5655–5663.

Haimeur, A., Brochu, C., Genest, P., Papadopoulou, B., Ouellette, M., 2000. Amplification of the ABC transporter gene PGPA and increased trypanothione levels in potassium antimonyl tartrate (SbIII) resistant *Leishmania tarentolae*. Mol. Biochem. Parasitol. 108 (1), 131–135.

Iantorno, S.A., Durrant, C., Khan, A., Sanders, M.J., Beverley, S.M., Warren, W.C., et al., 2017. Gene expression in *Leishmania* is regulated predominantly by gene dosage. mBio 8 (5).

Imamura, H., Downing, T., Van den Broeck, F., Sanders, M.J., Rijal, S., Sundar, S., et al., 2016. Evolutionary genomics of epidemic visceral leishmaniasis in the Indian subcontinent. Elife 5.

Légaré, D., Cayer, S., Singh, A.K., Richard, D., Papadopoulou, B., Ouellette, M., 2001. ABC proteins of *Leishmania*. J. Bioenerg. Biomembr. 33 (6), 469–474.

Leprohon, P., Legare, D., Girard, I., Papadopoulou, B., Ouellette, M., 2006. Modulation of *Leishmania* ABC protein gene expression through life stages and among drug-resistant parasites. Eukaryot. Cell 5 (10), 1713–1725.

Leprohon, P., Legare, D., Raymond, F., Madore, E., Hardiman, G., Corbeil, J., et al., 2009a. Gene expression modulation is associated with gene amplification,

supernumerary chromosomes and chromosome loss in antimony-resistant *Leishmania infantum*. Nucleic Acids Res. 37 (5), 1387–1399.
Leprohon, P., Legare, D., Ouellette, M., 2009b. Intracellular localization of the ABCC proteins of *Leishmania* and their role in resistance to antimonials. Antimicrob. Agents Chemother. 53 (6), 2646–2649.
Leprohon, P., Fernandez-Prada, C., Gazanion, É., Monte-Neto, R., Ouellette, M., 2015. Drug resistance analysis by next generation sequencing in *Leishmania*. Int. J. Parasitol.: Drugs Drug Resistance 5 (1), 26–35.
Marciano, D., Santana, M., Mantilla, B.S., Silber, A.M., Marino-Buslje, C., Nowicki, C., 2010. Biochemical characterization of serine acetyltransferase and cysteine desulfhydrase from *Leishmania major*. Mol. Biochem. Parasitol. 173 (2), 170–174.
Marquis, N., Gourbal, B., Rosen, B.P., Mukhopadhyay, R., Ouellette, M., 2005. Modulation in aquaglyceroporin AQP1 gene transcript levels in drug-resistant *Leishmania*. Mol. Microbiol. 57 (6), 1690–1699.
McKenna, A., Hanna, M., Banks, E., Sivachenko, A., Cibulskis, K., Kernytsky, A., et al., 2010. The Genome Analysis Toolkit: a MapReduce framework for analyzing next-generation DNA sequencing data. Genome Res. 20 (9), 1297–1303.
do Monte-Neto, R.L., Coelho, A.C., Raymond, F., Legare, D., Corbeil, J., Melo, M.N., et al., 2011. Gene expression profiling and molecular characterization of antimony resistance in *Leishmania amazonensis*. PLoS Neglected Trop. Dis. 5 (5), e1167.
Monte-Neto, R., Laffitte, M.C., Leprohon, P., Reis, P., Frezard, F., Ouellette, M., 2015. Intrachromosomal amplification, locus deletion and point mutation in the aquaglyceroporin AQP1 gene in antimony resistant *Leishmania* (*Viannia) guyanensis*. PLoS Neglected Trop. Dis. 9 (2), e0003476.
Moreira, E.S., Anacleto, C., Petrillo-Peixoto, M.L., 1998. Effect of glucantime on field and patient isolates of New World Leishmania: use of growth parameters of promastigotes to assess antimony susceptibility. Parasitol. Res. 84 (9), 720–726.
Mukherjee, A., Padmanabhan, P.K., Singh, S., Roy, G., Girard, I., Chatterjee, M., et al., 2007. Role of ABC transporter MRPA, gamma-glutamylcysteine synthetase and ornithine decarboxylase in natural antimony-resistant isolates of *Leishmania donovani*. J. Antimicrob. Chemother. 59 (2), 204–211.
Mukherjee, A., Boisvert, S., Monte-Neto, R.L., Coelho, A.C., Raymond, F., Mukhopadhyay, R., et al., 2013. Telomeric gene deletion and intrachromosomal amplification in antimony-resistant *Leishmania*. Mol. Microbiol. 88 (1), 189–202.
Mukhopadhyay, R., Dey, S., Xu, N., Gage, D., Lightbody, J., Ouellette, M., et al., 1996. Trypanothione overproduction and resistance to antimonials and arsenicals in *Leishmania*. Proc. Natl. Acad. Sci. U. S. A. 93 (19), 10383–10387.
Mukhopadhyay, R., Mandal, G., Atluri, V.S., Figarella, K., Uzcategui, N.L., Zhou, Y., et al., 2011. The role of alanine 163 in solute permeability of *Leishmania major* aquaglyceroporin LmAQP1. Mol. Biochem. Parasitol. 175 (1), 83–90.
Ouellette, M., Papadopoulou, B., 1993. Mechanisms of drug resistance in *Leishmania*. Parasitol. Today 9 (5), 150–153.
Ouellette, M., Drummelsmith, J., Papadopoulou, B., 2004. Leishmaniasis: drugs in the clinic, resistance and new developments. Drug Resist. Updates 7 (4), 257–266.
Papadopoulou, B., Roy, G., Ouellette, M., 1992. A novel antifolate resistance gene on the amplified H circle of *Leishmania*. EMBO J. 11 (10), 3601–3608.
Papadopoulou, B., Roy, G., Dey, S., Rosen, B.P., Ouellette, M., 1994. Contribution of the *Leishmania* P-glycoprotein-related gene ltpgpA to oxyanion resistance. J. Biol. Chem. 269 (16), 11980–11986.
Papadopoulou, B., Roy, G., Dey, S., Rosen, B.P., Olivier, M., Ouellette, M., 1996. Gene disruption of the P-glycoprotein related gene pgpa of *Leishmania tarentolae*. Biochem. Biophys. Res. Commun. 224 (3), 772–778.
Patino, L.H., Imamura, H., Cruz-Saavedra, L., Pavia, P., Muskus, C., Mendez, C., et al., 2019. Major changes in chromosomal somy, gene expression and gene dosage driven by Sb(III) in *Leishmania braziliensis* and *Leishmania panamensis*. Sci. Rep. 9 (1), 9485.
Perry, M.R., Wyllie, S., Prajapati, V.K., Feldmann, J., Sundar, S., Boelaert, M., et al., 2011. Visceral leishmaniasis and arsenic: an ancient poison contributing to antimonial treatment failure in the Indian subcontinent? PLoS Neglected Trop. Dis. 5 (9), e1227.
Perry, M.R., Wyllie, S., Raab, A., Feldmann, J., Fairlamb, A.H., 2013. Chronic exposure to arsenic in drinking water can lead to resistance to antimonial drugs in a mouse model of visceral leishmaniasis. Proc. Natl. Acad. Sci. U. S. A. 110 (49), 19932–19937.
Plourde, M., Ubeda, J.M., Mandal, G., Monte-Neto, R.L., Mukhopadhyay, R., Ouellette, M., 2015. Generation of an aquaglyceroporin AQP1 null mutant in *Leishmania major*. Mol. Biochem. Parasitol. 201 (2), 108–111.
Ponte-Sucre, A., Gamarro, F., Dujardin, J.C., Barrett, M.P., Lopez-Velez, R., Garcia-Hernandez, R., et al., 2017. Drug resistance and treatment failure in leishmaniasis: a 21st century challenge. PLoS Neglected Trop. Dis. 11 (12), e0006052.
Rijal, S., Chappuis, F., Singh, R., Bovier, P.A., Acharya, P., Karki, B.M., et al., 2003. Treatment of visceral leishmaniasis in south-eastern Nepal: decreasing efficacy of sodium stibogluconate and need for a policy to limit further decline. Trans. R. Soc. Trop. Med. Hyg. 97 (3), 350–354.
Ritt, J.F., Raymond, F., Leprohon, P., Legare, D., Corbeil, J., Ouellette, M., 2013. Gene amplification and point mutations in pyrimidine metabolic genes in 5-fluorouracil resistant *Leishmania infantum*. PLoS Neglected Trop. Dis. 7 (11), e2564.
Singh, K., Singh, K.P., Equbal, A., Suman, S.S., Zaidi, A., Garg, G., et al., 2016. Interaction between cysteine synthase and serine O-acetyltransferase proteins and their stage specific expression in *Leishmania donovani*. Biochimie 131, 29–44.
Sterkers, Y., Lachaud, L., Crobu, L., Bastien, P., Pages, M., 2011. FISH analysis reveals aneuploidy and continual generation of chromosomal mosaicism in *Leishmania major*. Cell Microbiol. 13 (2), 274–283.
Sundar, S., Rai, M., 2002. Laboratory diagnosis of visceral leishmaniasis. Clin. Diagn. Lab. Immunol. 9 (5), 951–958.
Sundar, S., More, D.K., Singh, M.K., Singh, V.P., Sharma, S., Makharia, A., et al., 2000. Failure of pentavalent antimony in visceral leishmaniasis in India: report from the center of the Indian epidemic. Clin. Infect. Dis. 31 (4), 1104–1107.
Ubeda, J.M., Legare, D., Raymond, F., Ouameur, A.A., Boisvert, S., Rigault, P., et al., 2008. Modulation of gene expression in drug resistant *Leishmania* is associated with gene amplification, gene deletion and chromosome aneuploidy. Genome Biol. 9 (7), R115.
Vanaerschot, M., Decuypere, S., Berg, M., Roy, S., Dujardin, J.C., 2013. Drug-resistant microorganisms with a higher fitness–can medicines boost pathogens? Crit. Rev. Microbiol. 39 (4), 384–394.
WHO, 2013. Leishmaniases. In: Sustaining the Drive to Overcome the Global Impact of Neglected Tropical Diseases: Second WHO Report on Neglected Tropical Diseases [Internet]. World Health Organization (WHO), pp. 67–71.
Wyllie, S., Cunningham, M.L., Fairlamb, A.H., 2004. Dual action of antimonial drugs on thiol redox metabolism in the human pathogen *Leishmania donovani*. J. Biol. Chem. 279 (38), 39925–39932.
Zackay, A., Cotton, J.A., Sanders, M., Hailu, A., Nasereddin, A., Warburg, A., et al., 2018. Genome wide comparison of Ethiopian *Leishmania donovani* strains reveals differences potentially related to parasite survival. PLoS Genet. 14 (1), e1007133.